IL NUOVO CIMENTO Vol. 125 B, N. 5-6 Maggio-Giugno 2010
DOI 10.1393/ncb/i2010-10851-1

Basic topics: Special Issue

Quantum cascade laser-based photoacoustic sensor for environmental pollution monitoring

A. Elia(1), V. Spagnolo(1)(3), C. Di Franco(1), P. M. Lugarà(1)(2) and G. Scamarcio(1)(2)

(1) *CNR-IFN U.O.S. di Bari - via Amendola 173, 70126 Bari, Italy*
(2) *Dipartimento Interateneo di Fisica, Università di Bari - via Amendola 173 70126 Bari, Italy*
(3) *Dipartimento Interateneo di Fisica, Politecnico di Bari - via Amendola 173 70126 Bari, Italy*

(ricevuto il 14 Gennaio 2010; revisionato il 19 Febbraio 2010; approvato il 24 Febbraio 2010; pubblicato online il 7 Maggio 2010)

Summary. — We will report here on the design and realization of an optoacoustic sensor for trace gas detection. The sensor consists of a commercial quantum cascade laser and a resonant photoacoustic cell. Two different cell configurations have been investigated: a "standard" H-cell and an innovative T-cell. We will describe the results obtained in the detection of different gases, such as nitric oxide, which plays an important role in environmental pollution and in medical diagnostics, and formaldehyde, a gas of great interest for indoor and outdoor air pollution.

PACS 07.88.+y – Instruments for environmental pollution measurements.
PACS 42.62.Fi – Laser spectroscopy.
PACS 42.72.Ai – Infrared sources.
PACS 42.55.Px – Semiconductor lasers; laser diodes.

1. – Introduction

The detection of trace gases with concentrations in the parts in 10^9 (ppbv) and sub-ppbv range is of great interest in a wide range of applications such as pollution monitoring, toxic-gas detection, human breath analysis for medical diagnostics and industrial process control.

In recent years, the development of new mid-infrared laser sources, *i.e.* gas lasers (CO, CO_2), lead-salt diode lasers, coherent sources based on difference frequency generation, optical parametric oscillators, quantum and interband cascade lasers, has given a new impulse to infrared laser-based trace gas sensors. Among them, single-mode quantum cascade lasers (QCLs) have become very attractive for mid-infrared gas sensing techniques thanks to single-frequency operation, narrow linewidth, high powers at mid-IR

wavelengths (3 to 24 μm), room temperature and continuous wave (CW) operation [1]. They overcome some of the major drawbacks of other traditional mid-IR laser sources, *i.e.* lack of continuous wavelength tunability and large size and weight of gas lasers, large size and cooling requirement of lead salt diode lasers, complexity and low power of nonlinear optical sources.

In combination with these laser sources, photoacoustic spectroscopy (PAS) offers the advantage of high sensitivity (ppbv detection limits), large dynamic range, compact set-up, fast time-response and simple optical alignment, if compared with other more conventional spectroscopic detection schemes, such as multi-pass absorption spectroscopy, which offer similar performances but require more sophisticated equipments.

PAS is based on the generation of an acoustic wave in a resonant gas cell resulting from the absorption of modulated light of appropriate wavelength by molecules. The amplitude of this sound wave is directly proportional to the gas concentration and can be detected using a sensitive microphone if the laser beam is modulated in the audio frequency range [2].

We will describe here an optoacoustic sensor designed for the detection of two different gases: nitric oxide (NO) and formaldehyde (CH_2O).

The detection and quantification of NO play an important role in environmental pollution monitoring and in medical diagnostics. NO is formed during high-temperature combustion process, such as car exhaust, and it is implicated in the depletion of ozone layer and the generation of photochemical smog and acid rain [3]. More recently it has been demonstrated that NO is involved in biological functions and human pathologies. In particular, NO detection in human breath is important in non-invasive diagnostic of asthma and inflammatory lung diseases [4, 5].

CH_2O is considered a carcinogenic pollutant in the atmosphere and of concern in the indoor environment. CH_2O plays an important role in atmospheric chemistry, where it comes out as an intermediate species in the oxidation of most biogenic and anthropogenic hydrocarbons. It is also known as a primary emission product of incomplete hydrocarbon combustion [6], so represents an ubiquitous component of both remote and polluted urban atmospheric environments. The CH_2O concentrations in polluted urban environments are in the order of 10–20 ppbv, whereas in non-urban locations concentrations from 0.01 to 10 ppbv have been observed [7-10]. Moreover, formaldehyde is a chemical widely used in the manufacture of building materials and many household products like foams, consumer paints and polymer products. Outgassing of formaldehyde from these materials may lead to high CH_2O concentration levels in indoor air. Even at low concentrations, formaldehyde can lead to health risks and may be associated with various diseases, such as bronchial asthma, atopic dermatitis and "sick building" syndrome. At concentrations of 100–500 ppbv irritation of eyes, nose and throat has been reported. At higher concentrations CH_2O leads to headaches and dizziness, and at 100 ppmv (parts per million in volume) exposure can be fatal [11].

2. – Photoacoustic spectrometer

The standard approach to detecting the acoustic signal generated by the modulated laser radiation in a weakly absorbing gas utilizes an acoustic resonator [12-14].

The PA signal measured by the microphone is given by

$$S = C \cdot P(\lambda) \cdot \alpha(\lambda),$$

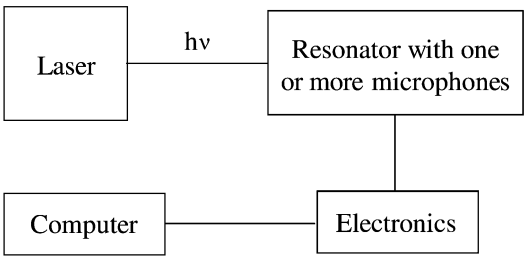

Fig. 1. – Typical PA spectrometer.

where C is the cell constant in the unit of Vcm/W, P the optical power of the laser source and α the absorption coefficient which is related to the gas concentration (N, number density of molecules) and absorption cross-section (σ) by $\alpha = N\sigma$. The cell constant depends on the geometry of the sample cell, the beam profile, the microphone response and the nature of the acoustic mode.

In our laboratories we have developed quantum cascade laser-based photoacustic sensors interesting for trace gas detection in pollution monitoring, industrial process control and medical diagnostic with a detection limit down to few tens of ppbv.

The optoacoustic sensors consist of a resonant cell, a commercially available distributed feedback quantum cascade laser source (QCL-DFB) and a signal acquisition and processing equipment. The light sources were supplied by Alpes Laser with drive electronics for pulsed operation at room temperature. A schematic diagram is shown in fig. 1.

The absorption of modulated laser radiation by molecules generates an acoustic signal in the cell, used for photoacoustic measurements. The PA signal can be amplified by tuning the modulation frequency to one of the acoustic resonances of the sample cell. In this resonant case the cell works as an acoustic amplifier; the absorbed laser power is accumulated in the acoustic mode of the resonator for Q oscillation periods, where Q is the quality factor, typically in the range of 10–300. The excited sound waves can be detected by one or more microphones and the microphones signal is measured by a lock-in amplifier.

Two types of resonant photoacoustic (PA) cell configurations have been investigated: a standard H-cell and an innovative T-cell.

2˙1. *H-cell.* – The resonant photoacoustic cell characterized by a H geometry consists of a cylindrical stainless-steel resonator of 120 mm length and 4 mm radius, with two 60 mm ($\lambda/4$) long buffer volumes connected to its endings in order to reduce by destructive interference the background signal, due to the heating of the two ZnSe windows, sealing the cell at its ends. To reduce the influence of adsorption/desorption processes at the inner surfaces of adhesive molecules, such as CH_2O and NO, a PA cell with gold-coated inner walls cell has been realized. The resonator, placed in a massive aluminum housing to minimize sensitivity to external noises, was designed to be excited in its first longitudinal mode at 1380 Hz; it was equipped with 4 electret microphones (Knowles EK 3024) with sensitivity of $S_m = 20$ mV/Pa, placed on the antinode of the acoustic mode to increase the signal-to-noise ratio. The electrical signal, fed by the microphones, was pre-amplified and then measured by a digital lock-in amplifier (EG&G Instruments) with a 10 s integration time constant. The laser radiation was collected with an AR-coated

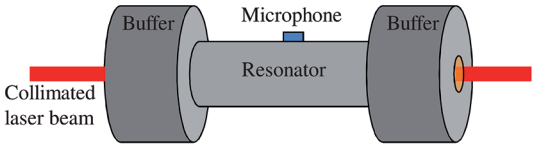

Fig. 2. – Schematic diagram of the photoacoustic H-cell.

ZnSe lens (2.54 cm focal length, $f/1$) and collimated by a beam condenser (0.2X) to avoid reflections on the cell walls. In fig. 2 we show a schematic of the H-cell.

In order to calculate the resonance frequency and the quality factor, we have measured the response of the cell in air using white noise as source. In fig. 3 the frequency response of the H-cell is reported; for our experiments we have selected the first longitudinal mode at 1380 Hz, showing a Q-factor of 45. The fundamental longitudinal eigenmode corresponds to that of a pipe with two open ends as reported in the inset of fig. 3.

2˙2. *T-cell.* – The resonant T-cell is characterized by a T geometry consisting of two intersecting volumes: an optical absorption volume and an acoustical resonance cylinder. This design allows independent optimization of the key parameters affecting the sensitivity of the PA sensor. The internal walls of the optical cavity have been shaped in order to produce multiple light reflection and subsequent focusing in the cavity center. We can change the resonator length and radius using a mechanical system in a range between 60–113 mm for the cylinder length and 8–12 mm for the internal diameter. At the end of the resonance cylinder an electret microphone (Knowles EK 3024) is mounted. This design does not require a collimated laser beam. This allows to use a mid-IR optical fiber to couple the laser source and the PA cell eliminating any optical alignment issue. The inner walls are gold coated in order to reduce adsorption/desorption effects of adhesive and highly polar molecules, such as CH_2O, on the walls of the PA cell. In fig. 4 a schematic of the T-cell is reported.

The electrical signal, fed by the microphone, was pre-amplified and measured by a digital lock-in, with a 10 s integration time constant.

We have studied the response of the T-cell in air as a function of the resonator length L using as source white noise. In fig. 5 the frequency response of the T-cell, corresponding to the fundamental longitudinal eigenmode of a pipe with one open and one close end,

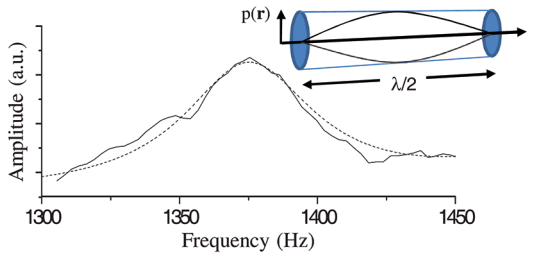

Fig. 3. – Response of the H-cell photoacoustic sensor to a white noise source. From the fit of the data (dotted line) we extract the resonance frequency and the related Q-factor. In the inset a schematic of the fundamental longitudinal eigenmode of the resonator (pipe with two open ends) is reported.

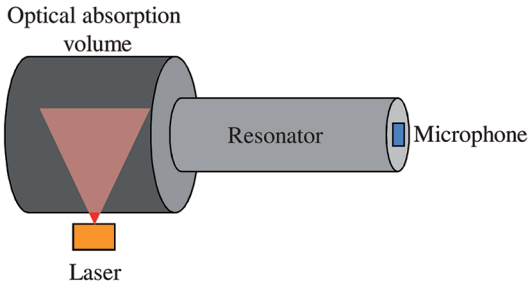

Fig. 4. – Schematic diagram of the photoacoustic T-cell.

for a cylinder length of 88 mm and a diameter of 12 mm is reported. This acoustic mode is characterized by a resonance frequency of 830 Hz with a Q-factor of 10. This results the best resonance configuration, in terms of quality factor, PA signal and immunity to external noise sources.

3. – Experimental results

Both the two PA sensors have been fully calibrated in terms of detection limit and minimum detectable absorption coefficient using certified gas mixtures [15, 16].

3˙1. *Formaldehyde*. – The laser used is a commercially available QC-DFB laser working in single-mode emission at a wavelength around 5.62 μm, where the formaldehyde C=O stretching mode (ν_2 fundamental band) is located [17].

For highly sensitive spectroscopic detection of CH_2O, suitable absorption lines characterized by high absorption intensity and free of cross-interferences of other gases have to be selected. Since strong absorption lines of H_2O fall in the spectral region of laser tunability, we performed an analysis of reference spectra of CH_2O and H_2O, obtained by ref. [18] and HITRAN database, respectively [19], in order to evaluate their possible interferences.

For PA detection of CH_2O we selected the absorption line at 1778.9 cm^{-1}, where we have a small overlap with water lines. This line is characterized by a strength of 5.68×10^{-20} cm/molecule. The lasing emission has been fixed over this line by setting the temperature of our QC laser at $T = 13.7\,^{\circ}C$. A certified 99.8-ppmv CH_2O in N_2

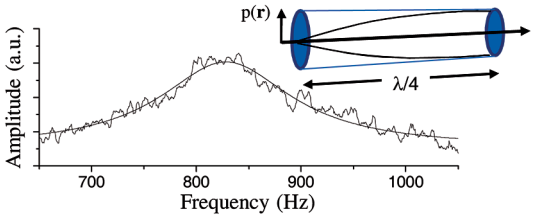

Fig. 5. – Response of the T-cell photoacoustic resonator to a white noise source, for a longitudinal resonator length of 88 mm. The resonance frequency and the related Q-factor were calculated from the fit of the data. In the inset the fundamental longitudinal eigenmode of the resonator (pipe with one open and one close end) is reported.

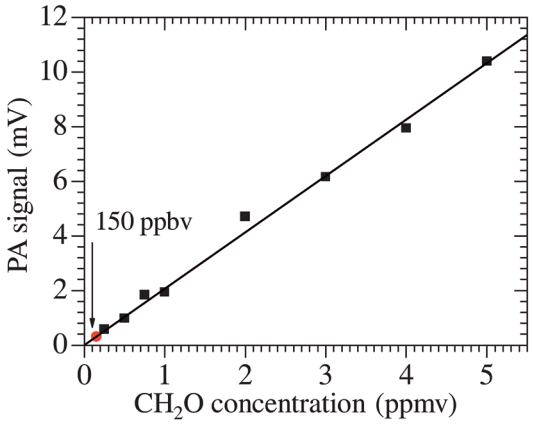

Fig. 6. – PA signal *vs.* CH_2O concentration measured using the H-cell. The symbols represent experimental data, the solid line is a linear fit. The vertical arrow marks the noise equivalent (signal-to-noise ratio of 1) minimum detection limit of 150 ppbv.

mixture was used to obtain known concentrations of the investigated gas via two mass flow controllers (Brooks Instrument). We use a chemical trap (Entegris mod. 35KF) to reduce the water vapour concentration in the certified mixture down to 0.1 ppbv. The pressure in the PA cell was kept at 1 bar. The background signal was measured by filling the PA cell with pure nitrogen and the electronic noise, due to electromagnetic noises and uncorrelated with the modulation frequency, was detected with the laser beam off. Each measurement was performed after an accurate purging of the cell to avoid contributions from adsorbed-desorbed molecules. The purging of the system was accomplished by a small vacuum diaphragm pump.

Figure 6 shows the PA signal measured using the H-cell as a function of CH_2O concentration and corrected for in-phase component of the background.

In fig. 7 preliminary results obtained with the alignment-free optoacoustic sensor based on the photoacoustic T-cell are reported.

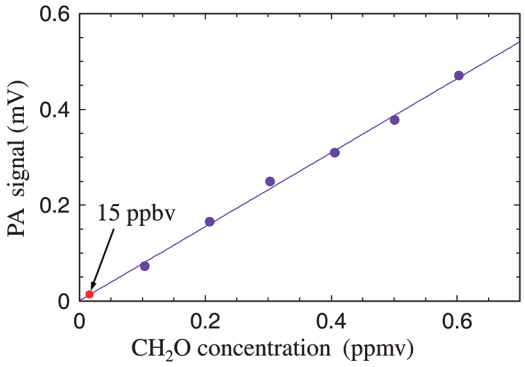

Fig. 7. – PA signal *vs.* CH_2O concentration measured using the T-cell. The symbols represent experimental data, the solid line is a linear fit. The arrow marks the noise equivalent (signal-to-noise ratio of 1) minimum detection limit of 15 ppbv.

TABLE I. – *H- and T-cell sensor performances.*

CH_2O	T-cell	H-cell
Detection limit (ppbv)	15	150
Min. det. abs. coefficient ($cm^{-1}\,W/Hz^{1/2}$)	1.6×10^{-9}	2.0×10^{-8}
α_{min} (cm^{-1})	5.2×10^{-8}	6.6×10^{-7}

In figs. 6 and 7, the solid lines are linear fits of the background-corrected data and show a strong linear relationship between the PA signal and the CH_2O concentration.

From the experimental data measured using the H- and T-cell we can extract the sensor detection limit and minimum detectable absorption coefficient, normalized to power and detection bandwidth. The detection limit was calculated by considering a signal-to-noise ratio (SNR) of 1 from the following equation:

$$C = \frac{SNR\sigma}{a},$$

where σ is the standard deviation of the linear fit and a the slope of the calibration curve (calibration factor). Sensors performance can be described also by the minimum detectable absorption coefficient, normalized to power and detection bandwidth:

$$D = \frac{\alpha_{min} P_0}{\sqrt{\Delta f}},$$

where α_{min} is the minimum detectable absorption coefficient at a SNR = 1, P_0 the average laser optical power and Δf the equivalent noise detection bandwidth.

In table I the H- and T-cell sensor performances are summarized. Both the detection limit and the minimum detectable absorption coefficient extracted for the T-cell configuration result about one order of magnitude better than those measured for the H-cell and this improvement results to be mainly due to the improved laser-cell coupling and to the reduction of the background signal obtained for the T configuration, which results also more compact and portable.

To quantify CH_2O concentrations, several laser-based spectroscopic sensors have been developed. One of the best results obtained was achieved using a more conventional spectroscopic detection scheme based on lead salt diode laser-based and a multipass optical cell with an effective optical path length of 100 m [20]. With this spectrometer detection of atmospheric formaldehyde was performed with a replicate precision < 0.050 ppbv for a 1 minute integration time, but cryogenically cooled laser light source and detector are required.

3˙2. *Nitric oxide.* – The light source used in this optoacoustic setup is a QC-DFB laser operating in pulsed mode at a wavelength around 5.34 μm. In order to maximize the laser power, limiting chirping effects, we worked with pulse duration of 42 ns and a duty cycle of 1.4%. The laser beam intensity was modulated by a mechanical chopper at the first longitudinal resonance frequency of the photoacoustic H-cell. For our sensor calibration we selected the P(1.5) NO lines located around 1871.06 cm^{-1}, having a maximum intensity of 0.8×10^{-20} cm/molecule. The lasing emission was tuned over these lines by setting the temperature of our QC laser at $T = 22\,^{\circ}C$. The concentration of NO was

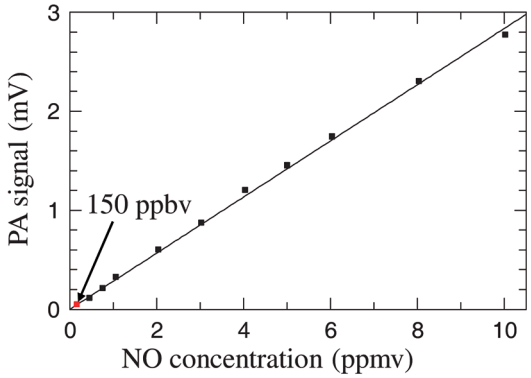

Fig. 8. – PA signal *vs.* NO concentration measured using the H-cell. The symbols represent experimental data, solid line is a linear fit. The arrow marks the noise equivalent (signal-to-noise ratio of 1) minimum detection limit of 150 ppbv.

reduced from 10 ppmv to 460 ppbv in steps and the magnitude of the photoacoustic signal was measured by the lock-in amplifier. Every time the gas concentration was changed, the working modulation frequency was optimized in order to follow the slight variation of cell resonance frequency. The background signal, mainly due to the periodical heating of the PA cell windows and walls, was measured by filling the PA cell with pure nitrogen; the noise, due to external acoustic and electromagnetic noises and mainly uncorrelated with the modulation frequency, was detected with the laser beam off.

Figure 8 shows the measured PA signal as a function of NO concentration corrected for in-phase component of the background. These measurements were performed after an accurate purging of the cell to avoid contributions from adsorbed-desorbed molecules. The solid line is a linear fit of the background-corrected data and shows a strong linear relationship ($r^2 \sim 0.99$) between the PA signal and the NO concentration. In this case we obtained from the experimental data a minimum detectable absorption coefficient of $1.3 \times 10^{-7}\,\mathrm{cm}^{-1}$, a minimum detectable absorption coefficient normalized to power and detection bandwidth of $2.0 \cdot 10^{-9}\,\mathrm{W} \cdot \mathrm{cm}^{-1}\,\mathrm{Hz}^{-1/2}$ and a detection limit of 150 ppbv.

Higher NO sensitivities were demonstrated with mid-IR spectrometers based upon a cw DFB QCL and a multiple-pass optical cell.

As an example, in 2006 Moeskops and co-workers [21] monitored the un-resolved NO-doublet at $1850.18\,\mathrm{cm}^{-1}$ using a single-mode thermoelectrically cooled cw QCL combined with wavelength modulation spectroscopy and an astigmatic multipass cell with an effective optical path of 76 m. They achieved a detection limit of 0.2 ppbv for NO in N2 with a 30 s integration time at 76 Torr. However, this sensitivity can only be reached with complex and bulky apparatus as multipass cell and cryogenically cooled low-noise detector which are of poor interest in the development of selective and sensitive optical sensors for field applications.

4. – Conclusions

PA trace gas sensors, based on a quantum cascade lasers, have been developed and calibrated. Two different resonant cells have been employed and the laser wavelengths have been carefully selected in order to achieve strong NO and CH_2O absorption, while

keeping the possible interferences from other species as low as possible. The PA sensors have been fully calibrated in terms of detection limit and minimum detectable absorption coefficient. A detection limit of 150 ppbv has been obtained for both the NO and CH_2O sensors using a H-cell configuration. Preliminary results obtained with the new PA cell characterized by a T geometry demonstrate that detection limit of few tens of ppbv and record normalized noise equivalent concentration in the range of $10^{-9}\,\mathrm{cm}^{-1}\,\mathrm{W/Hz}^{1/2}$ may be obtained; in particular, for CH_2O, a sensitivity improvement of one order of magnitude compared to the reported results with a conventional PA cell with H geometry has been obtained.

In addition to this, photoacoustic spectroscopy has the potentiality to result in simple, robust, cheaper and easy to maintain designs, less sensitive to the problems of interference fringes and optical misalignments, giving PAS a competitive advantage over other sensitive techniques and the possibility to obtain a man-portable sensor. In fact, although sub-ppbv CH_2O and NO detection sensitivities have been reported with the more conventional absorption spectroscopy in a multipass optical cell [20, 21], these techniques need sophisticated and/or cumbersome equipments, not suitable in applications which require compact and portable sensors. In particular, multi-pass absorption spectroscopy requires high-volume multi-pass cell and sensitive cryogenically cooled low-noise detectors.

* * *

The authors acknowledge partial financial support from Regione Puglia—Project DM01 related with the Apulian Technological District on Mechatronics—MEDIS.

REFERENCES

[1] Troccoli M., Diehl L., Bour D. P., Corzine S. W., Yu N., Wang C. Y., Belkin M. A., Höfler G., Lewicki R., Wysocki G., Tittel F. K. and Capasso F., *J. Lightwave Tech.*, **26** (2008) 3534.
[2] Sigrist M. W., *Air Monitoring by Spectroscopic Techniques* (Wiley, New York) 1994.
[3] Seinfeld J. H. and Pandis S. N., *Atmospheric Chemistry and Physics: From Air Pollution to Climate Change* (John Wiley & Sons, New York) 1998.
[4] Alving K., Weitzberg E. and Lundberg J. M., *Eur. Respir. J.*, **6** (1993) 1368.
[5] Wilson N. and Pedersen S., *Am. J. Respir. Crit. Care Med.*, **162** (2000) S48.
[6] Gbadebo Adewuyi Y., Cho S. Y., Tsay R. P. and Carmichael G. R., *Atmos. Environ.*, **18** (1984) 2413.
[7] Slemr J., *Fresenius J. Anal. Chem.*, **340** (1991) 672.
[8] Hanst P. L., Wong N. W. and Bragin J., *Atmos. Environ.*, **16** (1981) 969.
[9] Thomas W., Hegels E., Slijkhuis S., Spurr R. and Chance K., *Geophys. Res. Lett.*, **25** (1998) 1317.
[10] Yokelson R. J., Goode J. G., Ward D. E., Susott R. A., Babbitt R. E., Wade D. D., Bertschi I., Griffith D. W. T. and Hao W. M., *J. Geophys. Res. D*, **104** (1999) 30109.
[11] Chance K., Palmer P. I., Spurr R. J. D., Martin R. V., Kurosu T. P. and Jacob D. J., *Geophys. Res. Lett.*, **27** (2000) 3461.
[12] Lugarà P. M., Elia A. and Di Franco C., *Photoacoustic spectroscopy using semiconductor laser, in An Introduction to Optoelectronic Sensors – Series in Optics and Photonics*, Vol. **7**, edited by Righini G. C., Tajani A. and Cutolo A. (World Scientific; Singapore) 2009, pp. 257.
[13] Miklos A., Hess P. and Bozoki Z., *Rev. Sci. Instrum.*, **72** (2001) 1937.
[14] Elia A., Lugarà P. M., Di Franco C. and Spagnolo V., *Sensors*, **9** (2009) 9616.

[15] Elia A., Di Franco C., Spagnolo V., Lugarà P. M. and Scamarcio G., *Sensors*, **9** (2009) 2697.
[16] Di Franco C., Elia A., Spagnolo V., Scamarcio G., Lugarà P. M., Ieva E., Cioffi N., Torsi L., Bruno G., Losurdo M., Garcia M. A., Wolter S. D., Brown A. and Ricco M., *Sensors*, **9** (2009) 3337.
[17] Perrin A., Keller F. and Flaud J. M., *J. Mol. Spectrosc.*, **221** (2003) 192.
[18] Perrin A., Jacquemart D., Tchana F. K. and Lacome N., *J. Quant. Spectrosc. Rad. Transfer*, **110** (2009) 700.
[19] Available online: `http://www.hitran.com`.
[20] Wert B. P., Fried A., Rauenbuehler A. S., Walega J. and Henry B., *J. Geophys. Res.*, **108** (2003) 4350.
[21] Moeskops B., Cristescu S. and Harren F., *Opt. Lett.*, **31** (2006) 823.